Finite-difference scheme for a tensor PDE model of biological network formation and applications

Clarissa Astuto[(a)],
Daniele Boffi[(a),(b)], Jan Haskovec[(a)], Peter Markowich[(a),(c)], Giovanni Russo[(d)]
Vito Latora[(e),(d)], Claudio Caprioli[(d)]

February 21, 2023

(a) King Abdullah University of Science and Technology, Saudi Arabia
(b) University of Pavia
(c) University of Vienna
(d) University of Catania
(e) Queen Mary University of London

PRIN 2017: Innovative numerical methods for evolutionary partial differential equations and applications, final workshop
Dedicated to the memory of Maurizio Falcone
Catania 20-22 February 2023

Introduction and motivations

Introduction and motivations

Biological networks have been under scientific investigation for long time. We see immediate application in blood vasculature [1] and leaf venation.

Regarding leafs networks, the pattern of their venations seems to influence functionalities of the plant, such as its longevity, optimal water distribution and also the cells that are engaged in photosynthesis.

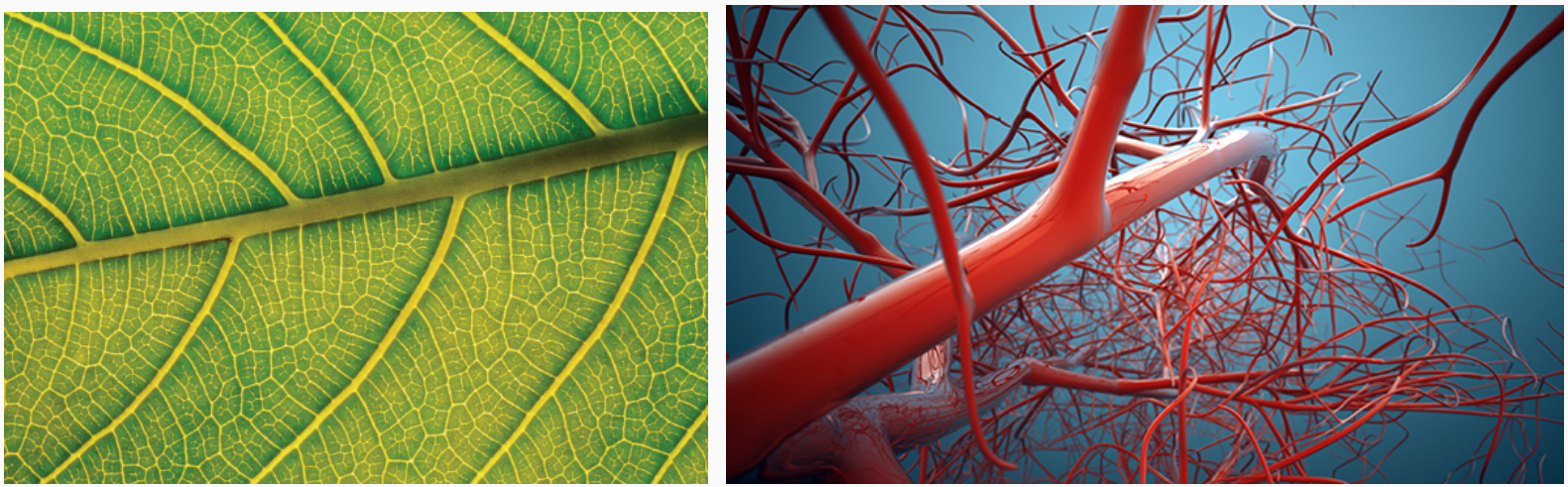

Figure 1: *Leaf venation (left), blood vasculature (right).*

[1] Hu, Cai and Rangan, Blood vessel adaptation with fluctuations in capillary flow distribution

We study the formation of network structures in biological systems. We consider a fluid moving through a porous medium, that is described by a Darcy's law for the pressure, which influences the movement of the fluid both in direction and intensity. The flux of the fluid is governed by the so-called permeability tensor $\mathbb{C}$, and vector m, whose action on the gradient of the pressure gives the direction of the flux. The permeability tensor usually depends on the conductivity of the medium, which describes how easy it is for the fluid to move in a point and what is the best direction to do so.

We study a continuous model which takes into consideration the evolution of the permeability tensor as a formal L2-gradient flow of an energy functional, consisting of a diffusion term, a metabolic and a kinetic term.

We study the formation of network structures in biological systems. We consider a fluid moving through a porous medium, that is described by a Darcy's law for the pressure, which influences the movement of the fluid both in direction and intensity. The flux of the fluid is governed by the so-called permeability tensor $\mathbb{C}$, and vector m, whose action on the gradient of the pressure gives the direction of the flux. The permeability tensor usually depends on the conductivity of the medium, which describes how easy it is for the fluid to move in a point and what is the best direction to do so.

We study a continuous model which takes into consideration the evolution of the permeability tensor as a formal L2-gradient flow of an energy functional, consisting of a diffusion term, a metabolic and a kinetic term.

About numerical schemes, we can find different papers:

- FD m-model: Di Fang, Shi Jin, P. Markowich and B. Perthame, 2019
- FEM m-model: G. Albi, M. Burger, J. Haskovec, P. Markowich, M. Schlottbom, 2017
- FEM m-model: G. Albi, M. Artina, M. Foransier and P. Markowich, 2016

Describing leaf venation phenomenon is very challenging because of the nature of the problem. Even in the same plant we can find different leafs with different venations patterns [2].

[2] Adaptation and optimization of biological transport networks, Hu Dan and Cai David, Physical review letters, 2013

Describing leaf venation phenomenon is very challenging because of the nature of the problem. Even in the same plant we can find different leafs with different venations patterns [2].

It becomes hard to compare numerical results when the features are very detailed. If the scales are not well solved, we can find differences when changing the parameters.

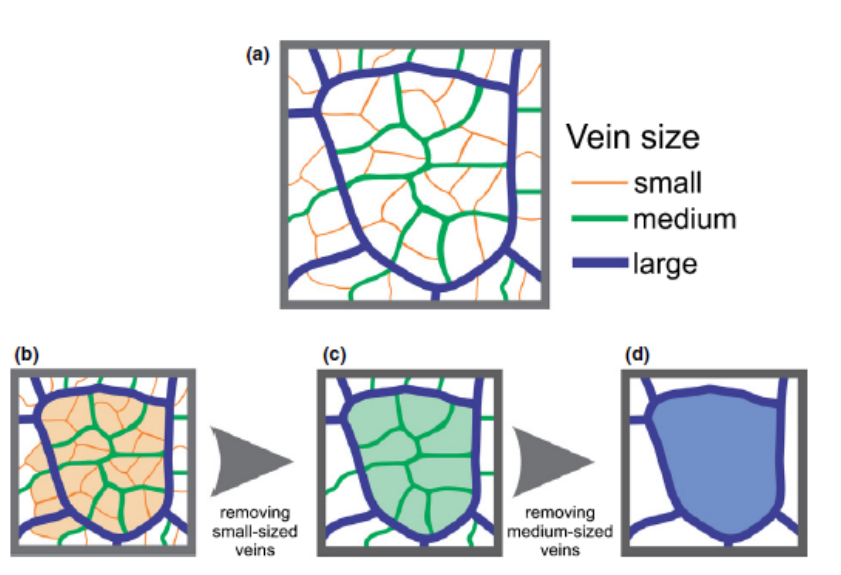

Figure 2: *Multiscale patterns.*

[2] Adaptation and optimization of biological transport networks, Hu Dan and Cai David, Physical review letters, 2013

Cai-Hu model [4],[5] - tensor $\mathbb{C}$-model

We refer to the Cai-Hu model to describe the formation of biological transport network.

$$-\nabla \cdot ((r\mathbb{I} + \mathbb{C})\nabla p) = S \tag{1}$$

$$\frac{\partial \mathbb{C}}{\partial t} - D^2 \Delta \mathbb{C} - c^2 \nabla p \otimes \nabla p + \frac{M'(\mathbb{C})}{|\mathbb{C}|}\mathbb{C} = 0 \tag{2}$$

- $p = p(t, \vec{x}) \in \mathbb{R}$ scalar pressure $\Longrightarrow$ pumping term
- $\mathbb{C} = \mathbb{C}(t, \vec{x}) \in \mathbb{R}^{2\times 2}$ conductance (permeability) tensor

The diffusion coefficient D controls the random effects, c is an activation parameter, r is the isotropic background permeability of the medium[3] and $S = S(\vec{x})$ the source function.

[3] Haskovec, Markowich, and Perthame. Mathematical analysis of a pde system for biological network formation, 2016.

[4] Adaptation and optimization of biological transport networks, Hu and Cai, 2013

[5] An optimization principle for initiation and adaptation of biological transport networks, Hu and Cai, 2019

The expression we choose for the metabolic function is

$$M(|\mathbb{C}|) := \frac{\alpha}{\gamma}|\mathbb{C}|^{\gamma} \quad \Longrightarrow \quad M'(|\mathbb{C}|) = \alpha|\mathbb{C}|^{\gamma-2} \tag{3}$$

as in [6],[7], where γ is the relaxation exponent and for leaf venation $1/2 < \gamma < 1$[8].

It represents the material cost of an edge of the network and it is proportional to a power of the conductance $\mathbb{C}$ of the edge, under the assumption that the total material cost of the network is constant.

[6] Biological transportation networks: Modeling and simulation, Albi G., Artina M., Foransier M. and Markowich P., Analysis and Applications, 2016

[7] Haskovec J., Markowich P. and Pilli G., Tensor PDE model of biological network formation, Communications in Mathematical Sciences, 2022

[8] Adaptation and optimization of biological transport networks, Hu Dan and Cai David, Physical review letters, 2013

The expression we choose for the metabolic function is

$$M(|\mathbb{C}|) := \frac{\alpha}{\gamma}|\mathbb{C}|^{\gamma} \quad \Longrightarrow \quad M'(|\mathbb{C}|) = \alpha|\mathbb{C}|^{\gamma-2} \tag{3}$$

as in [6],[7], where γ is the relaxation exponent and for leaf venation $1/2 < \gamma < 1$[8].

It represents the material cost of an edge of the network and it is proportional to a power of the conductance $\mathbb{C}$ of the edge, under the assumption that the total material cost of the network is constant.
At the end the model is

$$-\nabla \cdot ((r\mathbb{I} + \mathbb{C})\nabla p) = S \tag{4}$$

$$\frac{\partial \mathbb{C}}{\partial t} - D^2\Delta\mathbb{C} - c^2\nabla p \otimes \nabla p + \alpha|\mathbb{C}|^{\gamma-2}\mathbb{C} = 0 \tag{5}$$

[6] Biological transportation networks: Modeling and simulation, Albi G., Artina M., Foransier M. and Markowich P., Analysis and Applications, 2016

[7] Haskovec J., Markowich P. and Pilli G., Tensor PDE model of biological network formation, Communications in Mathematical Sciences, 2022

[8] Adaptation and optimization of biological transport networks, Hu Dan and Cai David, Physical review letters, 2013

The Cai-Hu model refers to a global energy consumption in the sense that the equations derive from the L^2-gradient flow of the functional

$$\mathcal{E}_{\text{tens}}[\mathbb{C}] := \int_\Omega \frac{D^2}{2}|\nabla \mathbb{C}|^2 + c^2 \nabla p[\mathbb{C}] \cdot \mathbb{P}[\mathbb{C}] \nabla p[\mathbb{C}] + M(|\mathbb{C}|)\, d\Omega. \tag{6}$$

In[9] they make sure that the derivative in time of the energy functional is negative, thus the system reaches a steady state, as a minimal energy consumption.

[9] Haskovec J., Markowich P. and Perthame B., Mathematical Analysis of a PDE System for Biological Network Formation, 2016

The Cai-Hu model refers to a global energy consumption in the sense that the equations derive from the L^2-gradient flow of the functional

$$\mathcal{E}_{\text{tens}}[\mathbb{C}] := \int_\Omega \frac{D^2}{2}|\nabla \mathbb{C}|^2 + c^2 \nabla p[\mathbb{C}] \cdot \mathbb{P}[\mathbb{C}] \nabla p[\mathbb{C}] + M(|\mathbb{C}|)\, d\Omega. \tag{6}$$

In[9] they make sure that the derivative in time of the energy functional is negative, thus the system reaches a steady state, as a minimal energy consumption.
To obtain the vector model for m, we consider the following energy functional:

$$(\text{ansatz}) \quad \mathbb{C} := \mathrm{m} \otimes \mathrm{m} \implies |\mathbb{C}| = |\mathrm{m}|^2$$

$$\mathcal{E}_{\text{vect}}[m] := \int_\Omega D^2 |\nabla m|^2 + c^2 \nabla p[m] \cdot \mathbb{P}[m \otimes m] \nabla p[m] + M(|m|^2) \mathrm{d}x. \tag{7}$$

[9] Haskovec J., Markowich P. and Perthame B., Mathematical Analysis of a PDE System for Biological Network Formation, 2016

Vector m-model

Taking the L^2-gradient flow with respect to the vector variable m of $\mathcal{E}_{\text{vect}}[m]$

$$-\nabla \cdot ((r\mathbb{I} + m \otimes m)\nabla p) = S \tag{8}$$

$$\frac{\partial m}{\partial t} - D^2 \Delta m - c^2(\nabla p \otimes \nabla p)m + \alpha |m|^{2(\gamma-1)} m = 0. \tag{9}$$

[10] Tensor PDE model of biological network formation, J. Haskovec, P. Markowich, G. Pilli, Communications in Mathematical Sciences

Vector m-model

Taking the L^2-gradient flow with respect to the vector variable m of $\mathcal{E}_{\text{vect}}[m]$

$$-\nabla \cdot ((r\mathbb{I} + m \otimes m)\nabla p) = S \tag{8}$$

$$\frac{\partial m}{\partial t} - D^2 \Delta m - c^2(\nabla p \otimes \nabla p)m + \alpha |m|^{2(\gamma-1)} m = 0. \tag{9}$$

Remark: The metabolic term $\alpha|\mathbb{C}|^{\gamma-2}\mathbb{C}$ becomes singular at $\mathbb{C} = 0$ if (and only if) $\gamma < 1$. This obviously causes difficulties for the $\mathbb{C}$-model [10].

[10] Tensor PDE model of biological network formation, J. Haskovec, P. Markowich, G. Pilli, Communications in Mathematical Sciences

Vector m-model

Taking the L^2-gradient flow with respect to the vector variable m of $\mathcal{E}_{\text{vect}}[m]$

$$-\nabla \cdot ((r\mathbb{I} + m \otimes m)\nabla p) = S \tag{8}$$

$$\frac{\partial m}{\partial t} - D^2 \Delta m - c^2(\nabla p \otimes \nabla p)m + \alpha |m|^{2(\gamma-1)} m = 0. \tag{9}$$

Remark: The metabolic term $\alpha|\mathbb{C}|^{\gamma-2}\mathbb{C}$ becomes singular at $\mathbb{C} = 0$ if (and only if) $\gamma < 1$. This obviously causes difficulties for the $\mathbb{C}$-model [10].

We are on a bounded domain $\Omega \subset \mathbb{R}^2$ with boundary conditions in $\partial\Omega$:

$$m(t, \vec{x}) = 0, \quad \mathbb{C}(t, \vec{x}) = 0, \quad \mathbb{P}\nabla p(t, \vec{x}) \cdot \nu = 0, \quad \vec{x} \in \partial\Omega,\ t \geq 0$$

where ν is the outgoing normal vector to $\partial\Omega$.

[10] Tensor PDE model of biological network formation, J. Haskovec, P. Markowich, G. Pilli, Communications in Mathematical Sciences

Numerical schemes

Space discretization

The domain is $\Omega = [0,1] \times [0,1]$, that we discretize by a uniform Cartesian mesh with spatial step $h := \Delta x = \Delta y$. The variables conductivity and pressure are $\mathbb{C}_{ij} \approx \mathbb{C}(x_i, y_j)$ and $p_{ij} \approx p(x_i, y_j)$.

Space discretization

The domain is $\Omega = [0,1] \times [0,1]$, that we discretize by a uniform Cartesian mesh with spatial step $h := \Delta x = \Delta y$. The variables conductivity and pressure are $\mathbb{C}_{ij} \approx \mathbb{C}(x_i, y_j)$ and $p_{ij} \approx p(x_i, y_j)$.

In order to obtain second order accuracy in space, we use central difference for the computation of the space derivatives:

$$\begin{aligned}
\frac{\partial m^{(1)}}{\partial t} &= D^2 \mathcal{L}\, m^{(1)} + c^2 \left(\mathcal{D}_x p\right)^2 m^{(1)} + c^2 \mathcal{D}_x p \mathcal{D}_y p\, m^{(2)} - \alpha |m|^{2(\gamma-1)} m^{(1)} \\
\frac{\partial m^{(2)}}{\partial t} &= D^2 \mathcal{L}\, m^{(2)} + c^2 \left(\mathcal{D}_y p\right)^2 m^{(2)} + c^2 \mathcal{D}_x p \mathcal{D}_y p\, m^{(1)} - \alpha |m|^{2(\gamma-1)} m^{(2)}
\end{aligned}$$

$$\frac{\partial C^{(1,1)}}{\partial t} = D^2 \mathcal{L}\, C^{(1,1)} + c^2 \left(\mathcal{D}_x p\right)^2 - \alpha |\mathbb{C}|^{\gamma-2} C^{(1,1)} \tag{10}$$

$$\frac{\partial C^{(1,2)}}{\partial t} = D^2 \mathcal{L}\, C^{(1,2)} + c^2 \mathcal{D}_x p \mathcal{D}_y p - \alpha |\mathbb{C}|^{\gamma-2} C^{(1,2)} \tag{11}$$

$$\frac{\partial C^{(2,2)}}{\partial t} = D^2 \mathcal{L}\, C^{(2,2)} + c^2 \left(\mathcal{D}_y p\right)^2 - \alpha |\mathbb{C}|^{\gamma-2} C^{(2,2)} \tag{12}$$

where $\mathbb{C}^{(1,2)} = \mathbb{C}^{(2,1)}$ ($\mathbb{C}$ is symmetric).

stabilization parameter for the reaction term

We introduce a 'small' parameter ε in the reaction term[11], as follows

$$\mathcal{Q}(\mathbb{C})\mathbb{C} = |\mathbb{C} + \varepsilon|^{\gamma-2}\mathbb{C} \tag{13}$$

and we study the behaviour of the system for $\varepsilon \to 0$.

[11] C. A., D. Boffi, J. Haskovec, P. Markowich and G. Russo, Comparison of two aspects of a PDE model for biological network formation, Mathematical and Computational Applications, 2022

stabilization parameter for the reaction term

We introduce a 'small' parameter ε in the reaction term[11], as follows

$$\mathcal{Q}(\mathbb{C})\mathbb{C} = |\mathbb{C} + \varepsilon|^{\gamma-2}\mathbb{C} \tag{13}$$

and we study the behaviour of the system for $\varepsilon \to 0$.

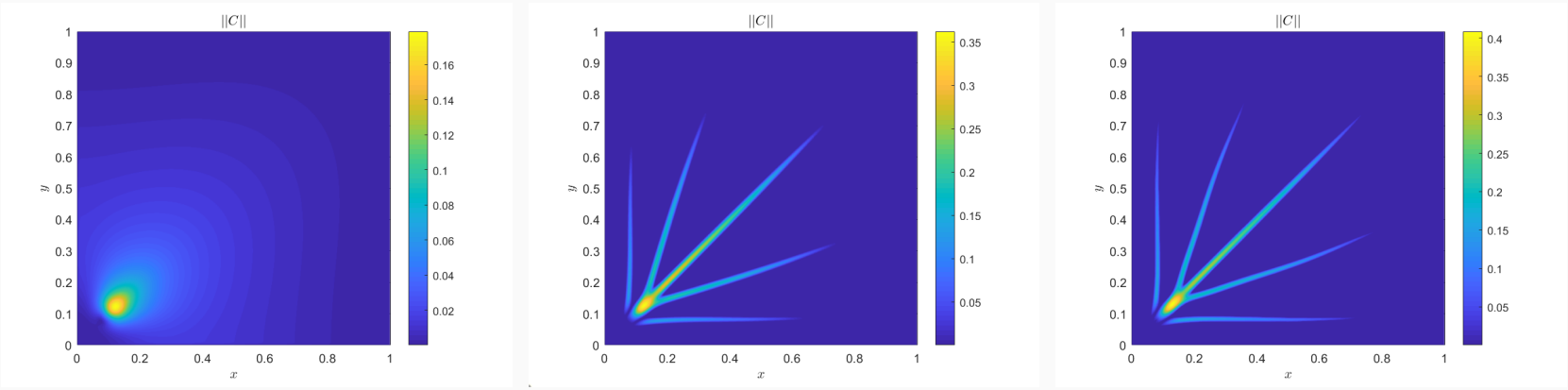

Figure 3: *On the left we have* $\varepsilon = 10^{-2}$, *center* $\varepsilon = 10^{-3}$ *and right* $\varepsilon = 10^{-4}$.

[11] C. A., D. Boffi, J. Haskovec, P. Markowich and G. Russo, Comparison of two aspects of a PDE model for biological network formation, Mathematical and Computational Applications, 2022

Time discretization - symmetric-ADI method

$\cdots$ we apply the symmetric-ADI method for the reaction-diffusion eq.

$$1^{st}\begin{cases}(\mathrm{y}-\mathrm{impl}) & \tilde{\mathbb{C}}_1 = \mathbb{C}^n + \frac{\Delta t}{2}\mathcal{L}_y\tilde{\mathbb{C}}_1 + \frac{\Delta t}{2}\mathcal{L}_x\mathbb{C}^n + \Delta t\,\mathcal{P}^{n+1/2} \\ (\mathrm{x}-\mathrm{impl}) & \mathbb{C}_y^{n+1} = \tilde{\mathbb{C}}_y + \frac{\Delta t}{2}\mathcal{L}_y\tilde{\mathbb{C}}_1 + \frac{\Delta t}{2}\mathcal{L}_x\mathbb{C}_y^{n+1} + \Delta t\,\mathcal{Q}\left(\mathbb{C}_y^{n+1}\right)\end{cases}$$

$$2^{nd}\begin{cases}(\mathrm{x}-\mathrm{impl}) & \tilde{\mathbb{C}}_2 = \mathbb{C}^n + \frac{\Delta t}{2}\mathcal{L}_y\mathbb{C}^n + \frac{\Delta t}{2}\mathcal{L}_x\tilde{\mathbb{C}}_2 + \Delta t\,\mathcal{P}^{n+1/2} \\ (\mathrm{y}-\mathrm{impl}) & \mathbb{C}_x^{n+1} = \tilde{\mathbb{C}}_x + \frac{\Delta t}{2}\mathcal{L}_y\mathbb{C}_x^{n+1} + \frac{\Delta t}{2}\mathcal{L}_x\tilde{\mathbb{C}}_2 + \Delta t\,\mathcal{Q}\left(\mathbb{C}_x^{n+1}\right)\end{cases}$$

$$\mathbb{C}^{n+1} = \frac{1}{2}\mathbb{C}_x^{n+1} + \frac{1}{2}\mathbb{C}_y^{n+1}$$

where $\mathcal{L}_\alpha$, with $\alpha = x, y$, are the discrete operators for the Laplacian in x and y direction respectively, with $\mathcal{L}_\alpha \in \mathbb{R}^{N\times N}$.

	ADI	sym-ADI
asymm($\mathbb{C}$)	0.1010	0.0031
asymm(p)	0.0248	0.0055

Table 1: $r = 10^{-3}, \varepsilon = r.$

	ADI	sym-ADI
asymm($\mathbb{C}$)	0.1199	0.0538
asymm(p)	0.0307	0.0021

Table 2: $r = 10^{-4}, \varepsilon = r.$

Accuracy tests

Accuracy tests: Richardson extrapolation

N	error_2	order	N	error_2	order
20	-	-	25	-	-
40	0.036012	-	50	9.066×10^{-2}	-
80	0.0493010	-0.4531	100	4.625×10^{-2}	0.97
160	0.01456192	1.7594	200	1.571×10^{-2}	1.56
320	0.00691103	1.0752	400	4.149×10^{-3}	1.92
640	0.001528055	2.1772	800	7.347×10^{-4}	2.50

Table 3: *Accuracy test of the m-system (left) and $\mathbb{C}$-system (right):* $\alpha = 0.5$, $c = 1$, $D = 0.01$, $\gamma = 0.75$, $r = 0.1$, $t_{\text{fin}} = 1$.

12

[12] C. A., D. Boffi, J. Haskovec, P. Markowich and G. Russo, Comparison of two aspects of a PDE model for biological network formation, Mathematical and Computational Applications, 2022

Accuracy tests: Wasserstein distance

The Wasserstein distance[13] of order $p = 2$ between μ and $\nu \in X$ metric space, where $\Pi(\mu, \nu)$ denotes the collection of all measures

$$\mathcal{W}_p(\mu, \nu) = \left(\inf_{\pi \in \Pi(\mu,\nu)} \int d(x, x_0)^p \, d\pi(x) \right)^{1/p}, \quad \int_X d(x, x_0)^p d\mu(x) < \infty$$

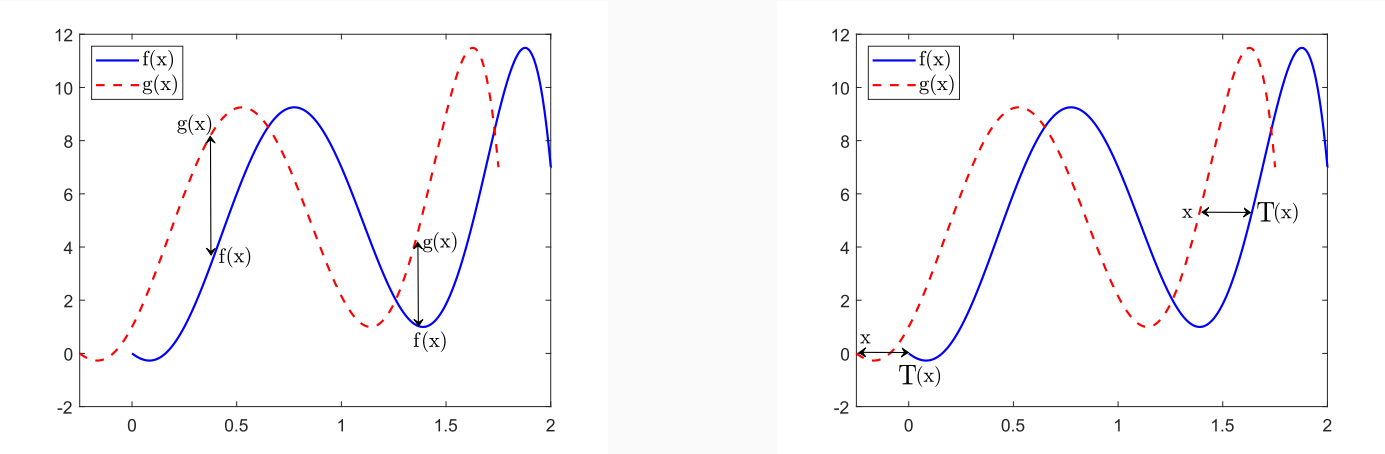

Figure 4: *'Vertical' vs 'horizontal' distances between a pair of functions: Wasserstein distance depends more on the displacement of the function than its shape.*

[14]

[13] The Wasserstein distances, Villani, 2009

[14] Euclidean, metric, and Wasserstein gradient flows: an overview, Santambrogio, 2017

Table 4: *Wasserstein distance,* $\text{error}_{\mathcal{W}}$ *vs Richardson extrapolation,* $\text{error}_{\mathcal{R}}$*: (left)* $r = 10^{-2}$ *and (right)* $r = 10^{-3}$*, at final time* $t = 3$*.*

N	$\text{error}_{\mathcal{W}}$	$\text{error}_{\mathcal{R}}$
100	-	-
200	3.846e-03	3.358e-01
400	9.579e-04	2.763e-01
800	1.8060e-04	2.199e-01

N	$\text{error}_{\mathcal{W}}$	$\text{error}_{\mathcal{R}}$
100	-	-
200	4.827e-03	3.273e-02
400	1.514e-03	3.292e-02
800	4.455e-04	2.609e-02

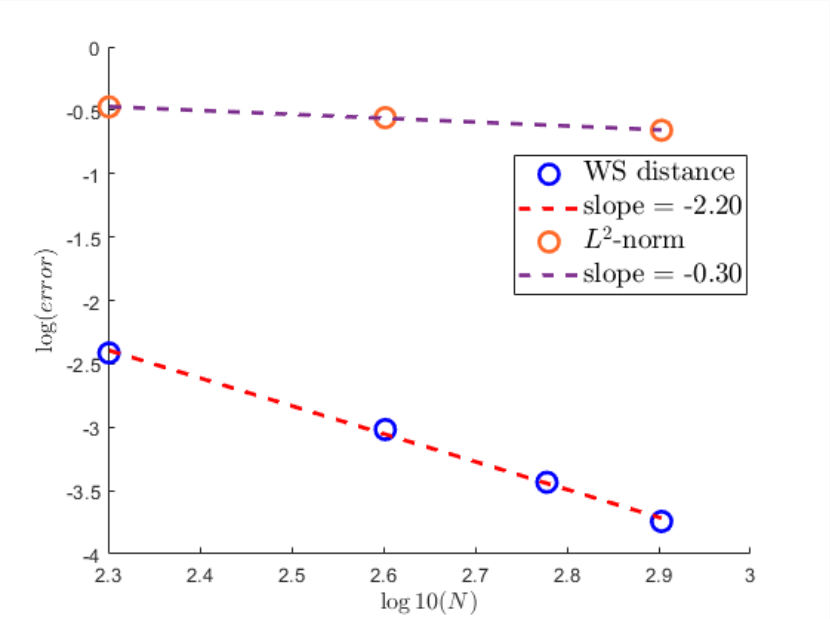

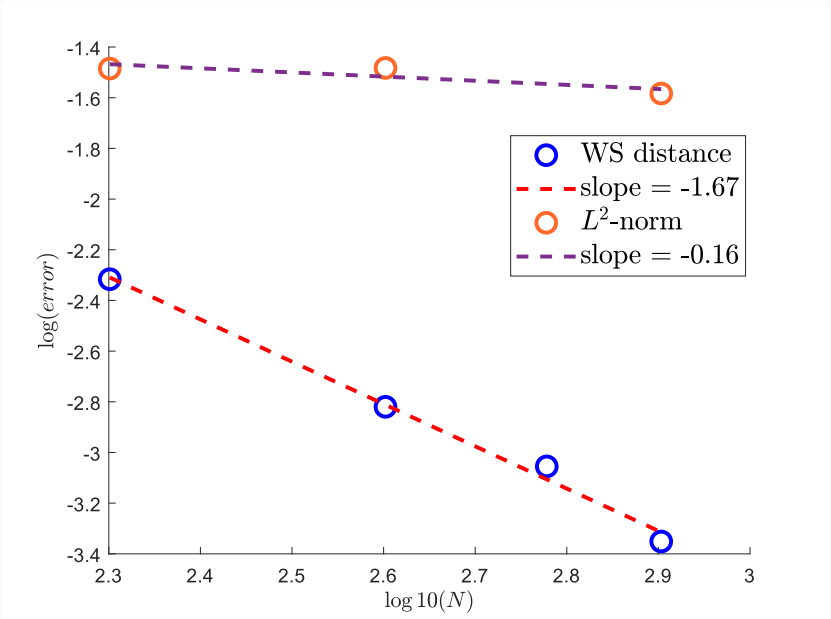

[15] A. C., Boffi, D. Haskovec, J. Markowich, P. and Russo, G., Asymmetry and condition number of an elliptic-parabolic system for biological network formation, 2023, arXiv

Validation I/II

$$m_1^{0,1} = 1, \quad m_2^{0,1} = \sqrt{2}; \quad m_1^{0,2} = 5, \quad m_2^{0,2} = 5;$$
$$m_1^{0,3} = (2 - |X + Y|)\exp(-10|X - Y|), \quad m_2^{0,3} = m_1^{0,3};$$

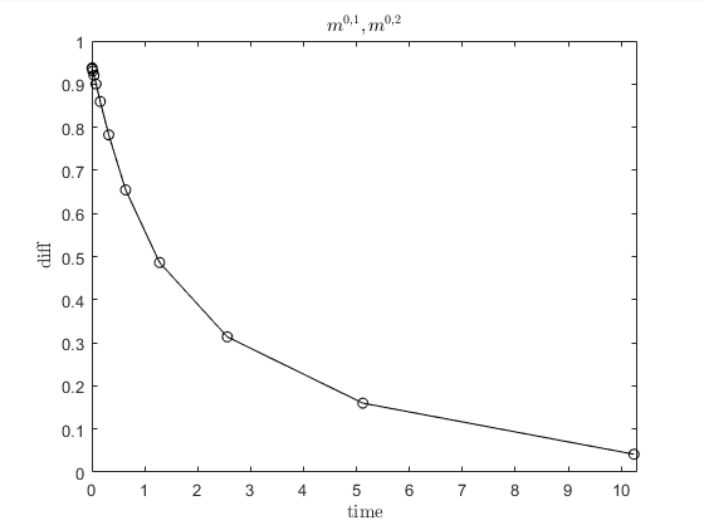

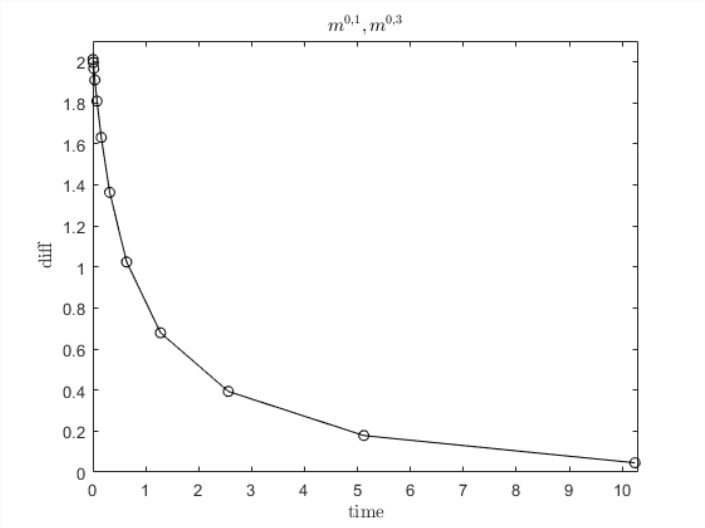

16

Figure 5: *Difference between two different solutions choosing, as initial condition,* $m^{0,1}, m^{0,2}$ *(on the left) and* $m^{0,1}, m^{0,3}$ *(on the right), with* $\gamma = 1.75 > 1$.

[16] Haskovec, Markowich, and Perthame. Mathematical analysis of a pde system for biological network formation, 2016.

Validation II/II

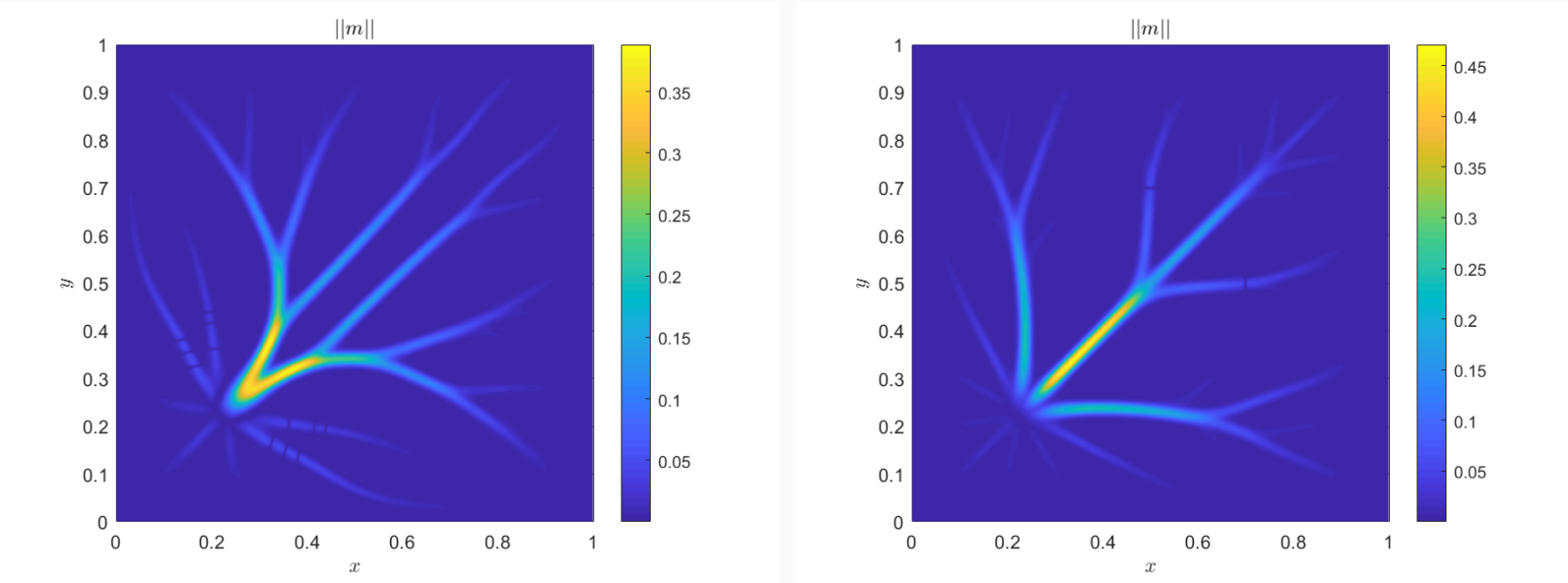

Figure 6: *In this figure we show the steady states when* $\gamma = 0.75 < 1$. *On the left the initial condition is* $m^0 = m^{0,1} = 1$ *while, on the right, the initial condition is a function of space,* $m^0 = m^{0,3}$.

Results

Results

$$m^0_{\text{comp}}(\vec{x}) = [1,1]^T, \qquad \mathbb{C}^0_{\text{comp}}(\vec{x}) = [1,0,1]^T, \qquad S(\vec{x}) = E - \bar{E}$$

$$E = \exp(-\sigma(\vec{x} - \vec{x}_0)^2),\ \bar{E} = \text{mean}(E),\ \sigma = 500,\ \vec{x}_0 = (0.25, 0.25)$$

$$\alpha = \gamma = 0.75, c = 5, D = 0.01, \varepsilon = 10^{-3}, r = 0.005, T = 15$$

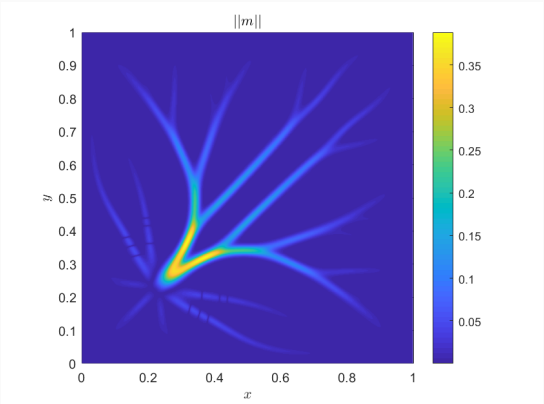

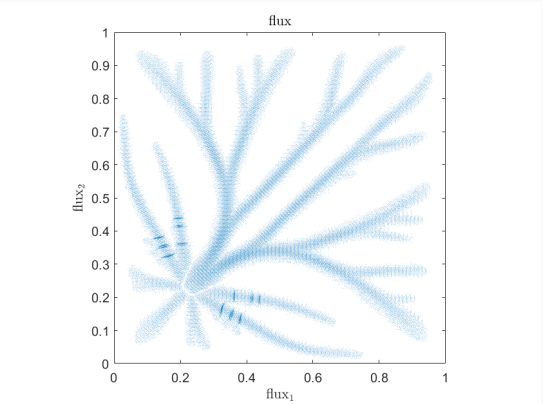

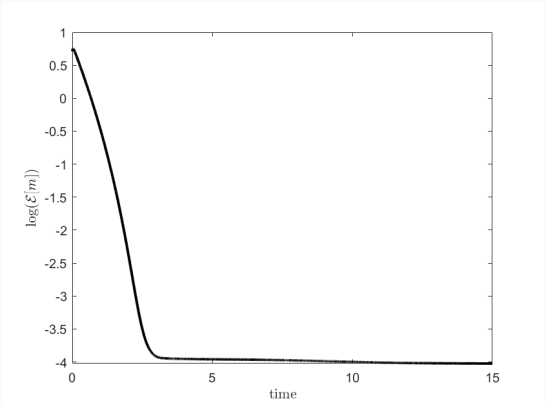

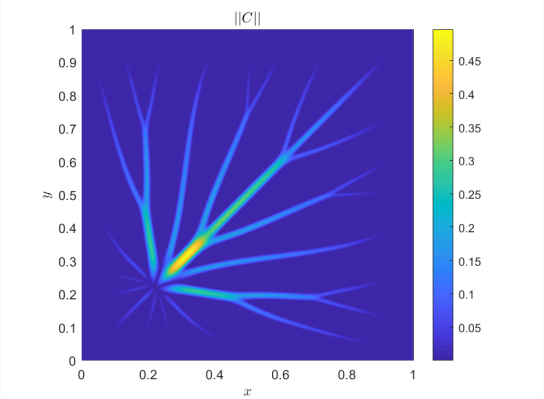

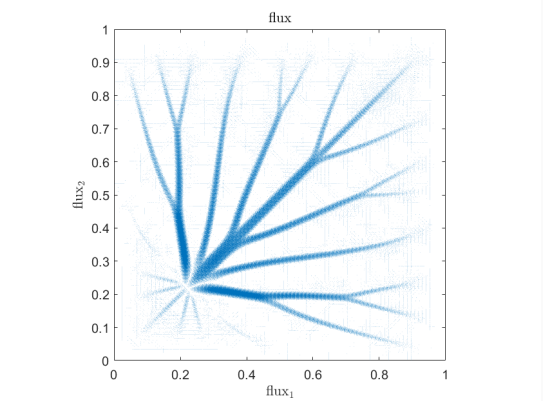

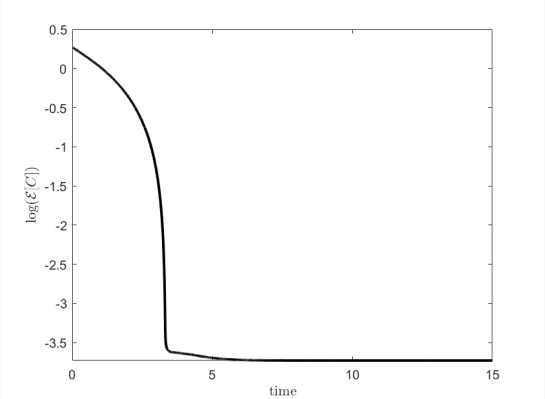

Tests on varying the diffusivity D

$$\alpha = \gamma = 0.75, c = 5, \varepsilon = 10^{-3}, r = 10^{-3}, T = 15$$

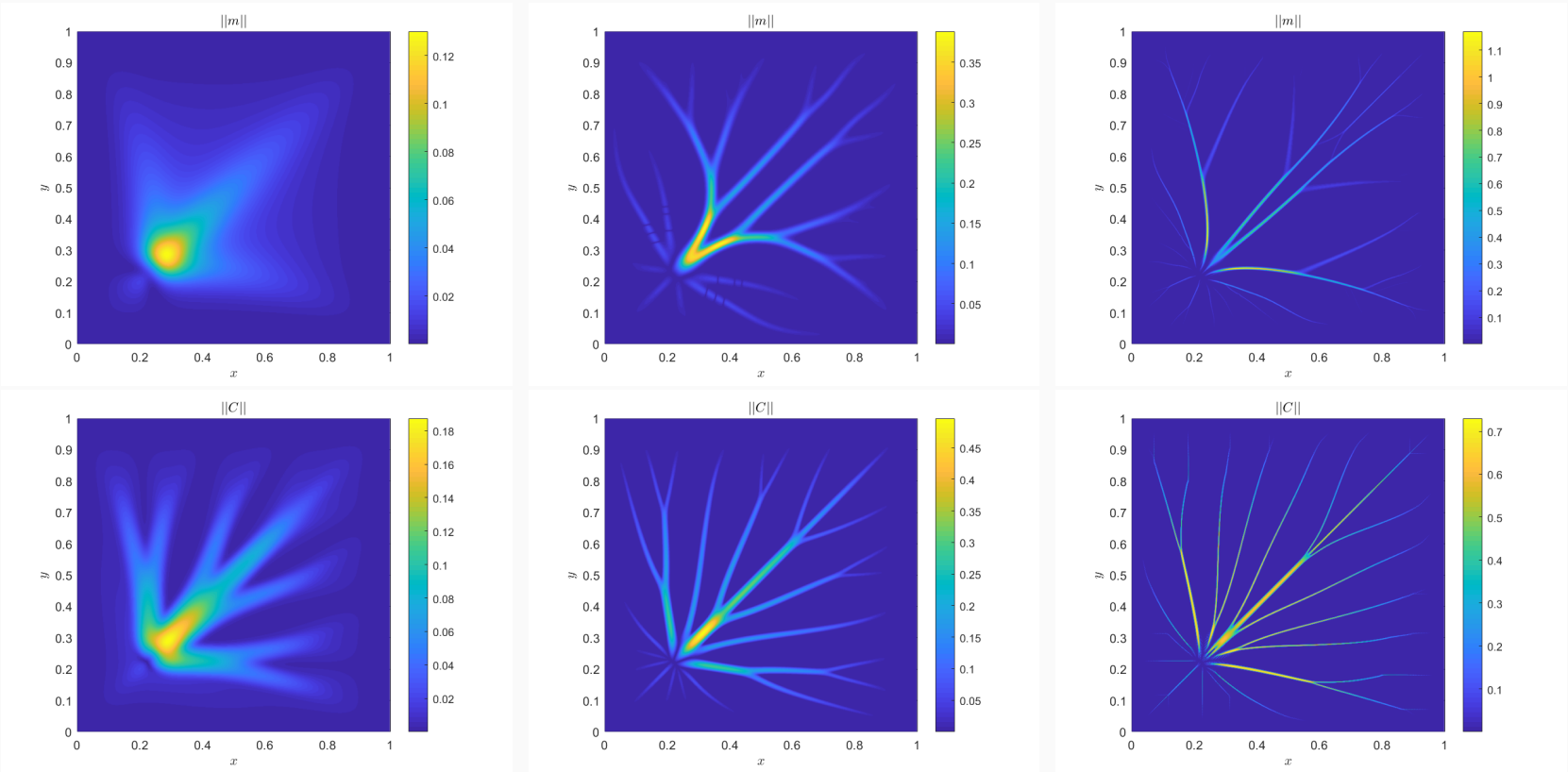

Figure 7: *$D = 0.05$ (left), $D = 0.01$ (center) and $D = 0.001$ (right).*

Tests varying the relaxation exponent γ

$$\alpha = \gamma = 0.75, c = 5, \varepsilon = 10^{-3}, r = 10^{-3}, T = 15$$

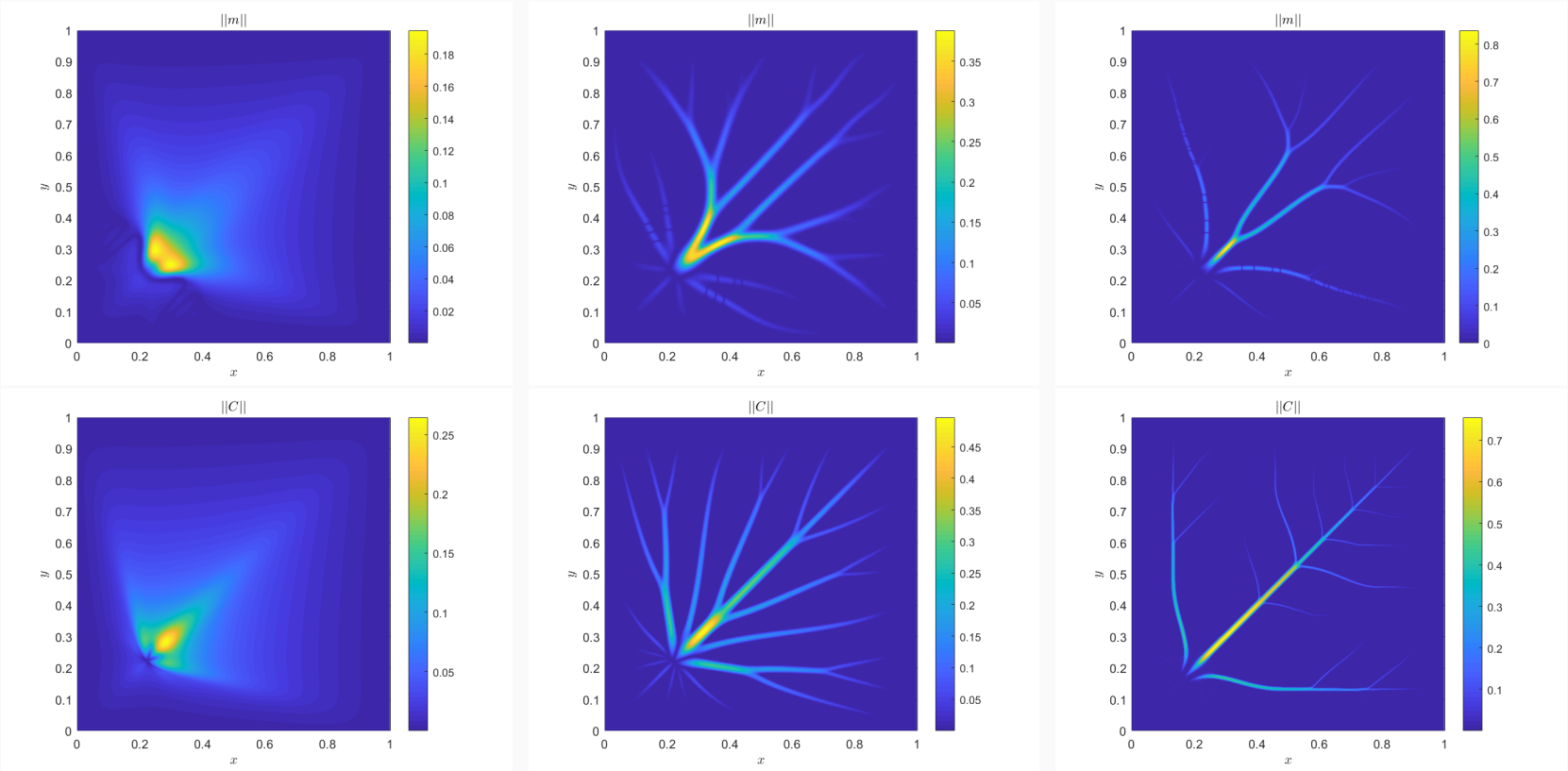

Figure 8: $\gamma = 0.95$ *(left)*, $\gamma = 0.75$ *(center)*, $\gamma = 0.55$ *(right)*.

Evolution in time of the solution

https://youtu.be/ENScpqNaTZU

Asymmetry and condition number and their dependence on the background permeability r

Asymmetry and condition number

In this section we compare the two versions of the ADI method to see the improvements in the symmetric version. We adopt a symmetric numerical scheme, and we choose symmetric initial datum and source function S. Consequently, the exact solution to the problem retains symmetry at each time step.

In order to check if our scheme is symmetric, we calculate the asymmetry of the solution with the following formula

$$\mathrm{asymm}(A) = \frac{||A - A^T||}{||A + A^T||}$$

	$r = 10^{-2}$		$r = 10^{-3}$		$r = 10^{-4}$	
	ADI	sym-ADI	ADI	sym-ADI	ADI	sym-ADI
asymm($\mathbb{C}$)	6.10e-04	4.39e-08	2.59e-02	1.67e-03	1.53e-01	1.86e-01
asymm(p)	3.88e-05	4.28e-09	6.13e-02	2.68e-03	2.68e-02	2.80e-02

Moreover, investigating the reasons why we lose the symmetry of the solution, we notice that it is related to the choice of the background permeability[17] r. When this parameters tends to zero, the condition number of the iteration matrix $\mathcal{L}$ increases, up to the order 10^8.

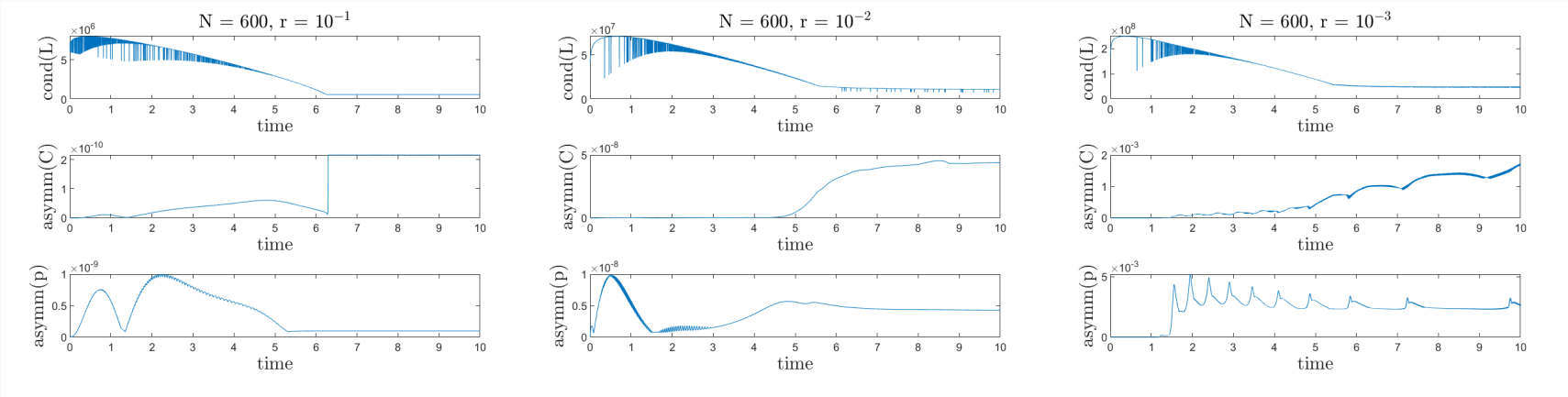

Figure 9: *Asymmetry of the module of the conductivity tensor $\mathbb{C}$ and the pressure p, as functions of time, together with the condition number of $\mathcal{L}$, for different values of $r = 10^{-1}, 10^{-2}, 10^{-3}$.*

[17] A. C., Boffi, D. Haskovec, J. Markowich, P. and Russo, G., Asymmetry and condition number of an elliptic-parabolic system for biological network formation, 2023, arXiv

changing r and constant initial condition

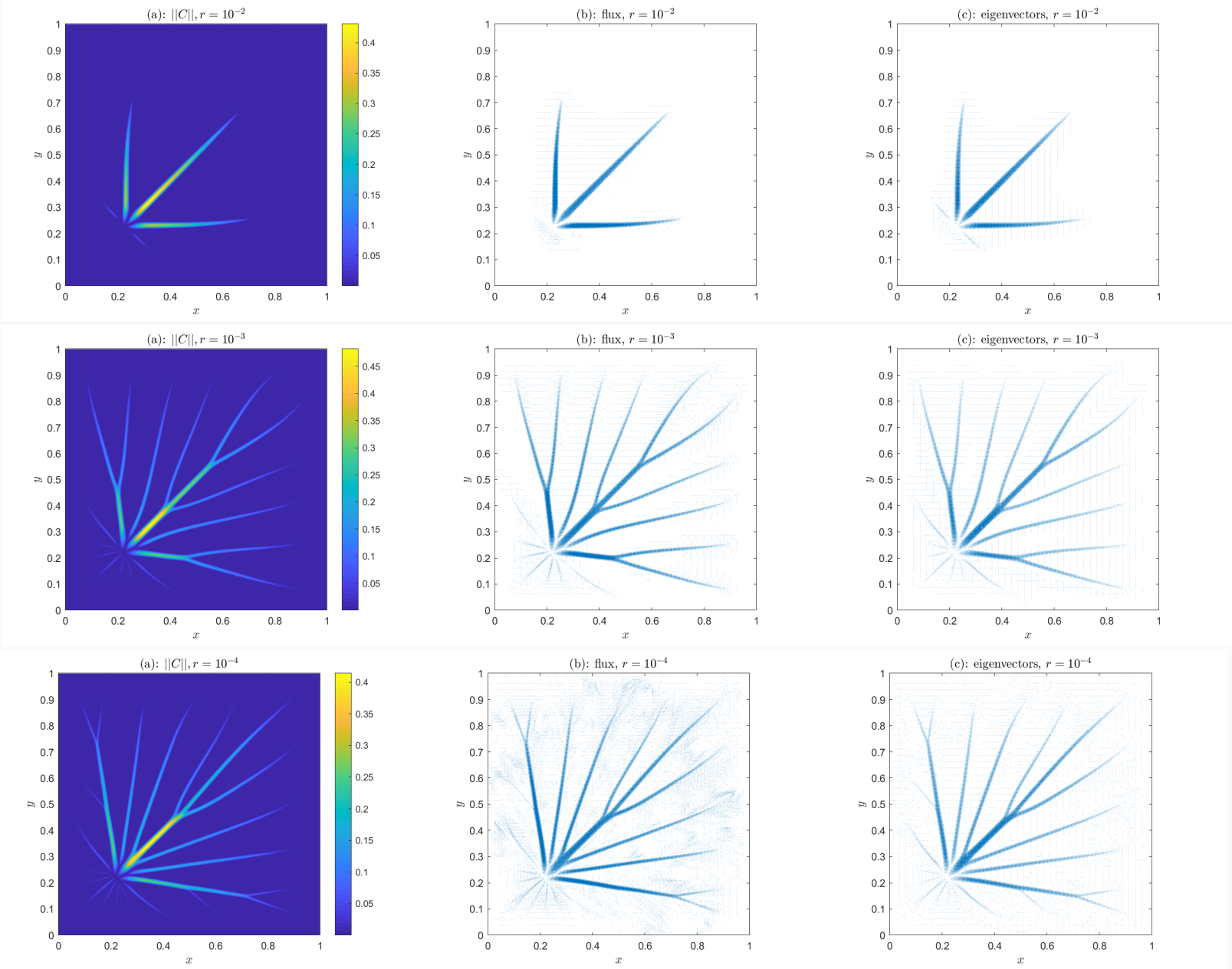

changing r and space dependent initial condition

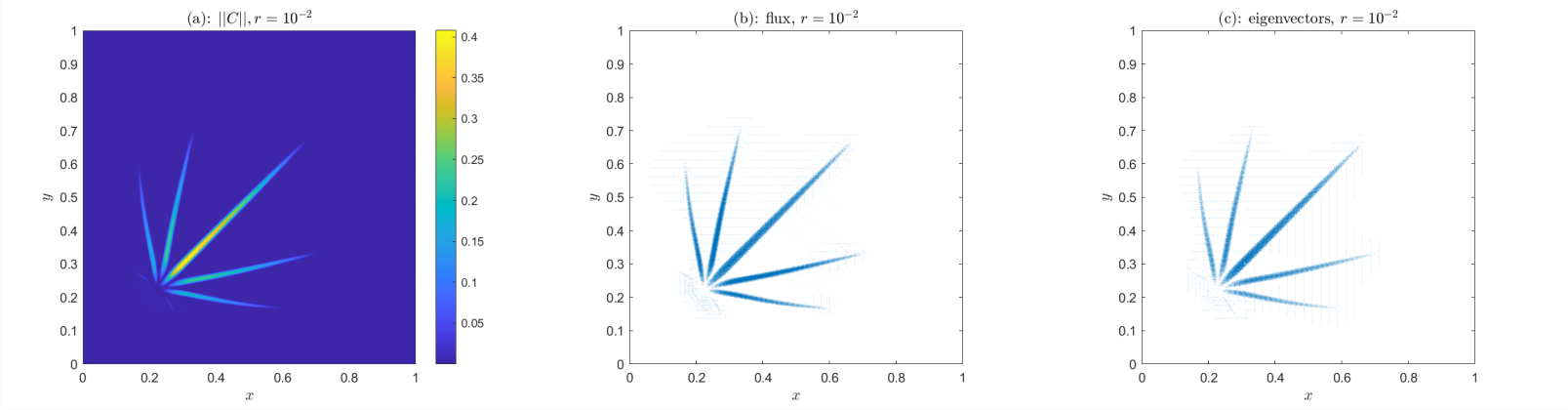

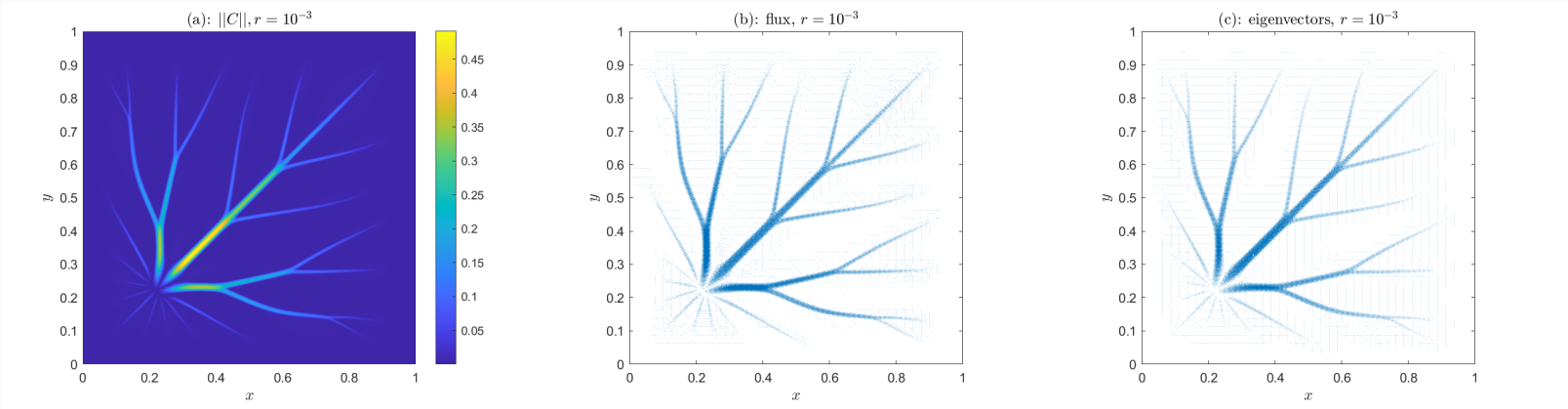

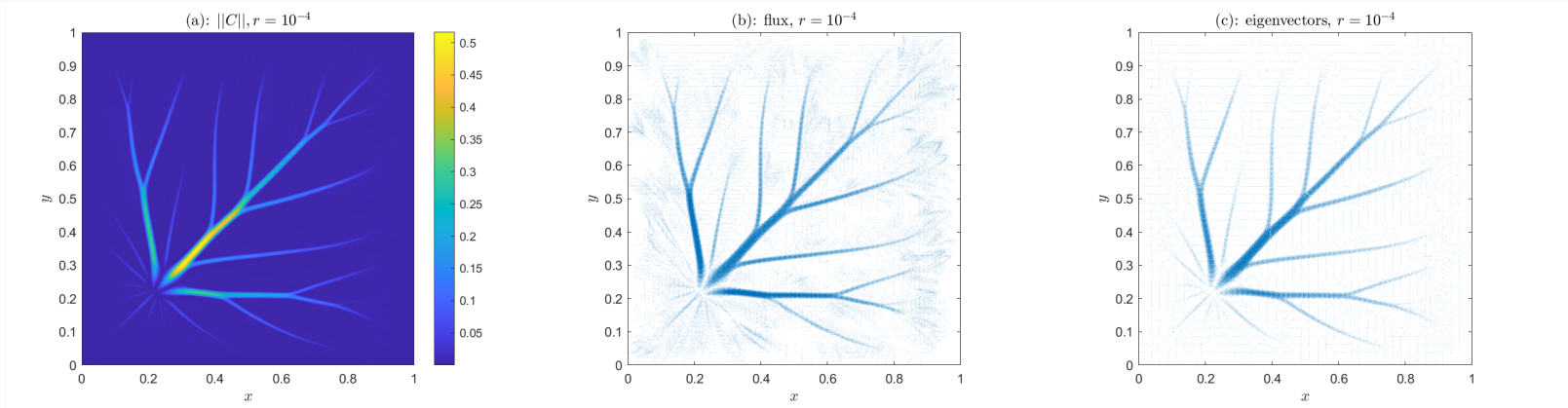

0-initial condition and 0-diffusivity

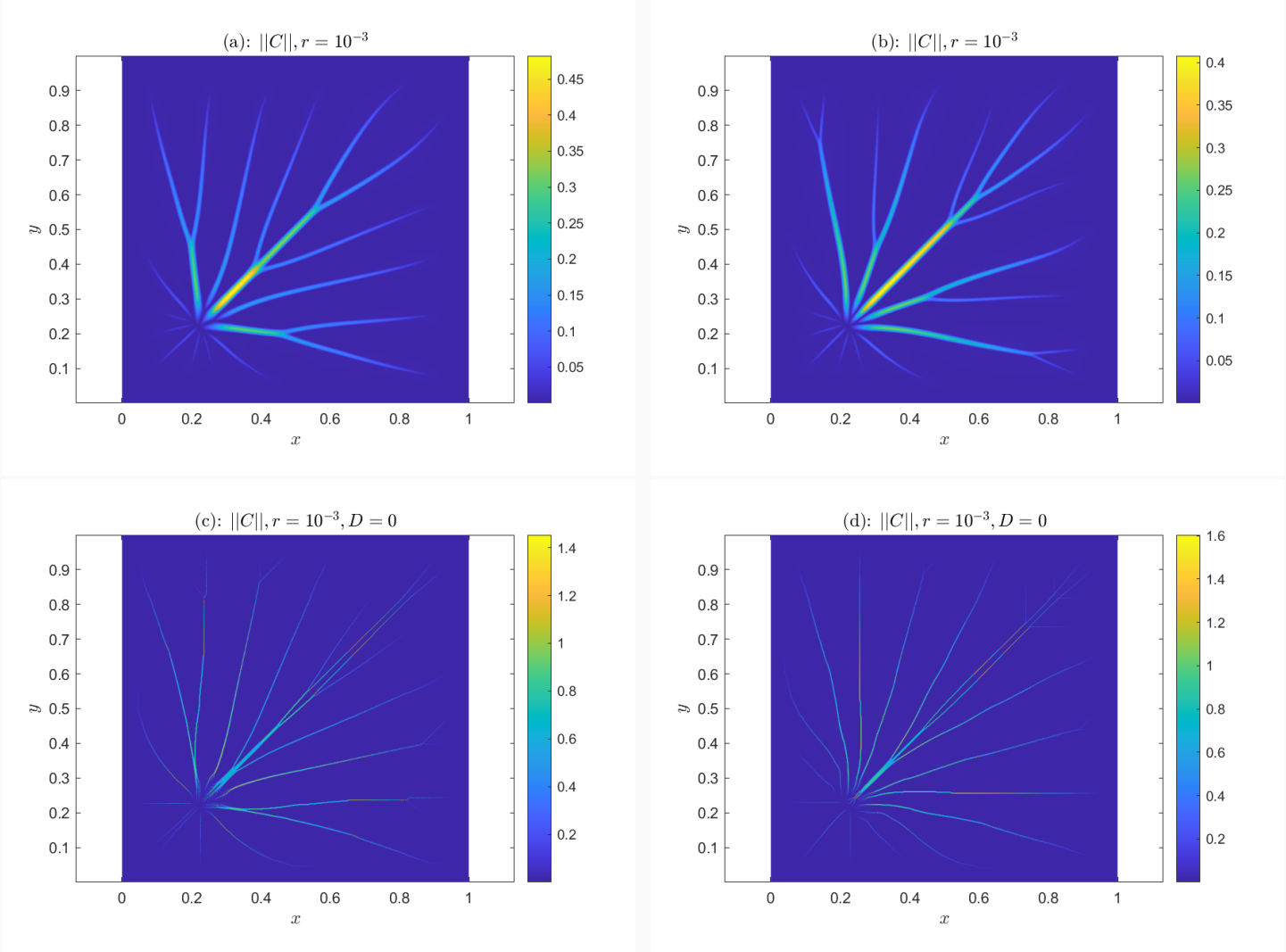

Figure 10: *In (a) and (c) the IC = 1, while in (b) and (d) we IC = 0. In plots (a) and (b) the diffusion coefficient is* $D = 10^{-2}$*, in (c) and (d)* $D = 0$*.*

Graph generation

Number of branches changing the activation parameter c

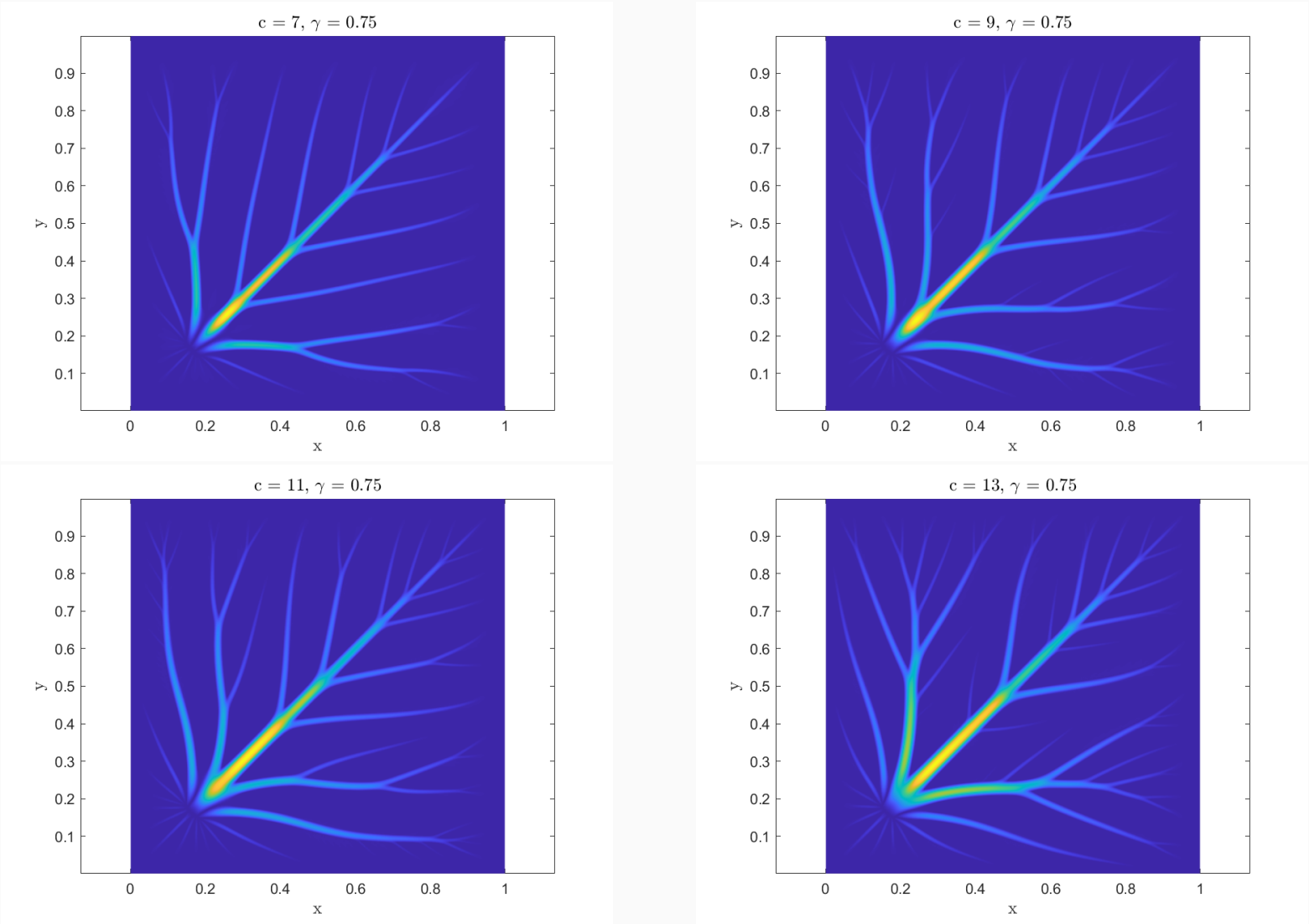

Figure 11: *Plot of $|\mathbb{C}|$. Results for different values of c, $\gamma = 0.75$.*

graph derived from the numerical solution

with python library `sknw`, starting from the numerical solution:

- **log** of the solution
- choosing an 'ad hoc' **threshold** (> 0) for the test
- **log** for the second time, to compress the solution and isolate the pixels with high intensity (close to 1)
- **binary** solution
- **skeleton**
- **graph**

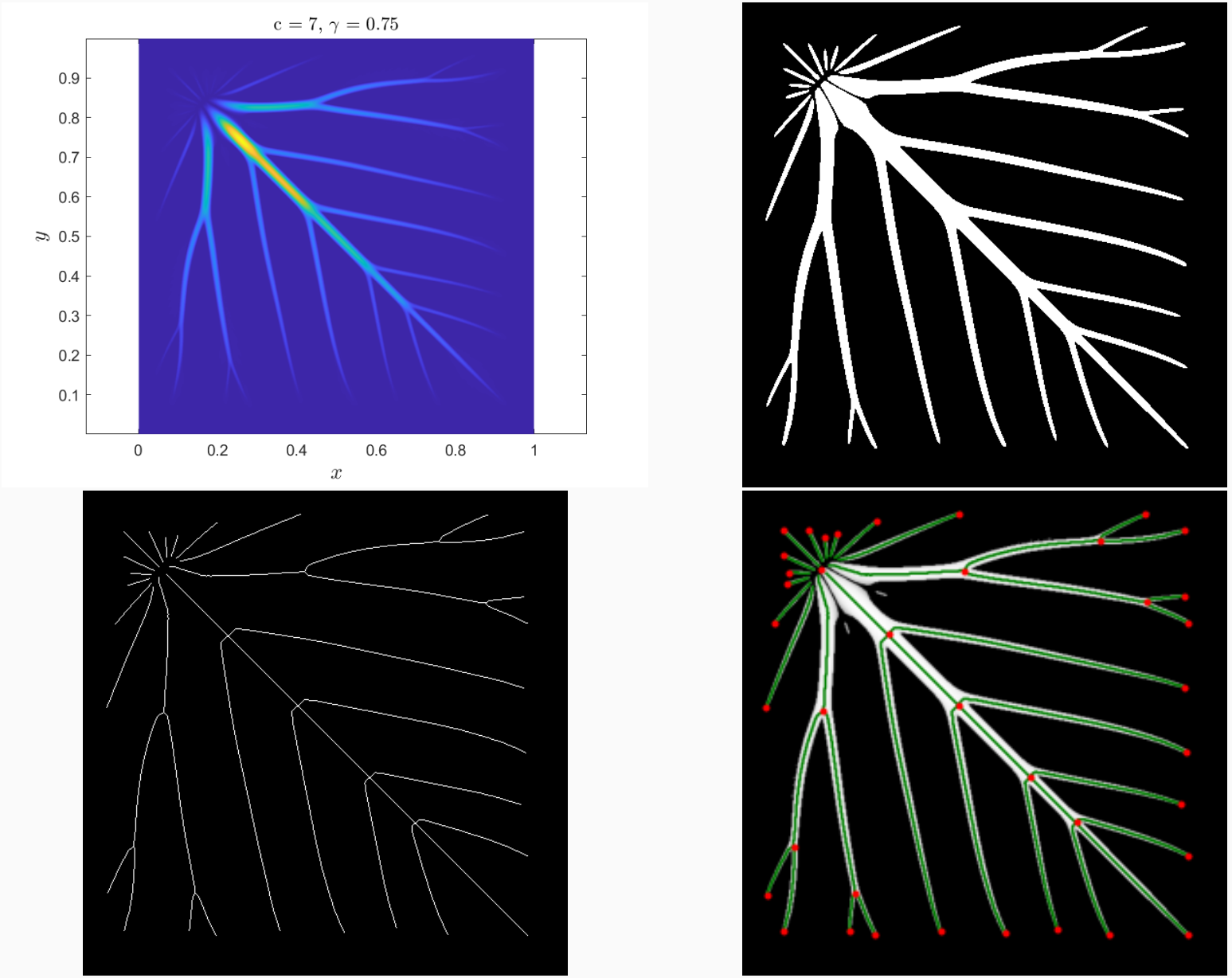

Figure 12: *Segmentation for* $c = 7, \gamma = 0.75$.

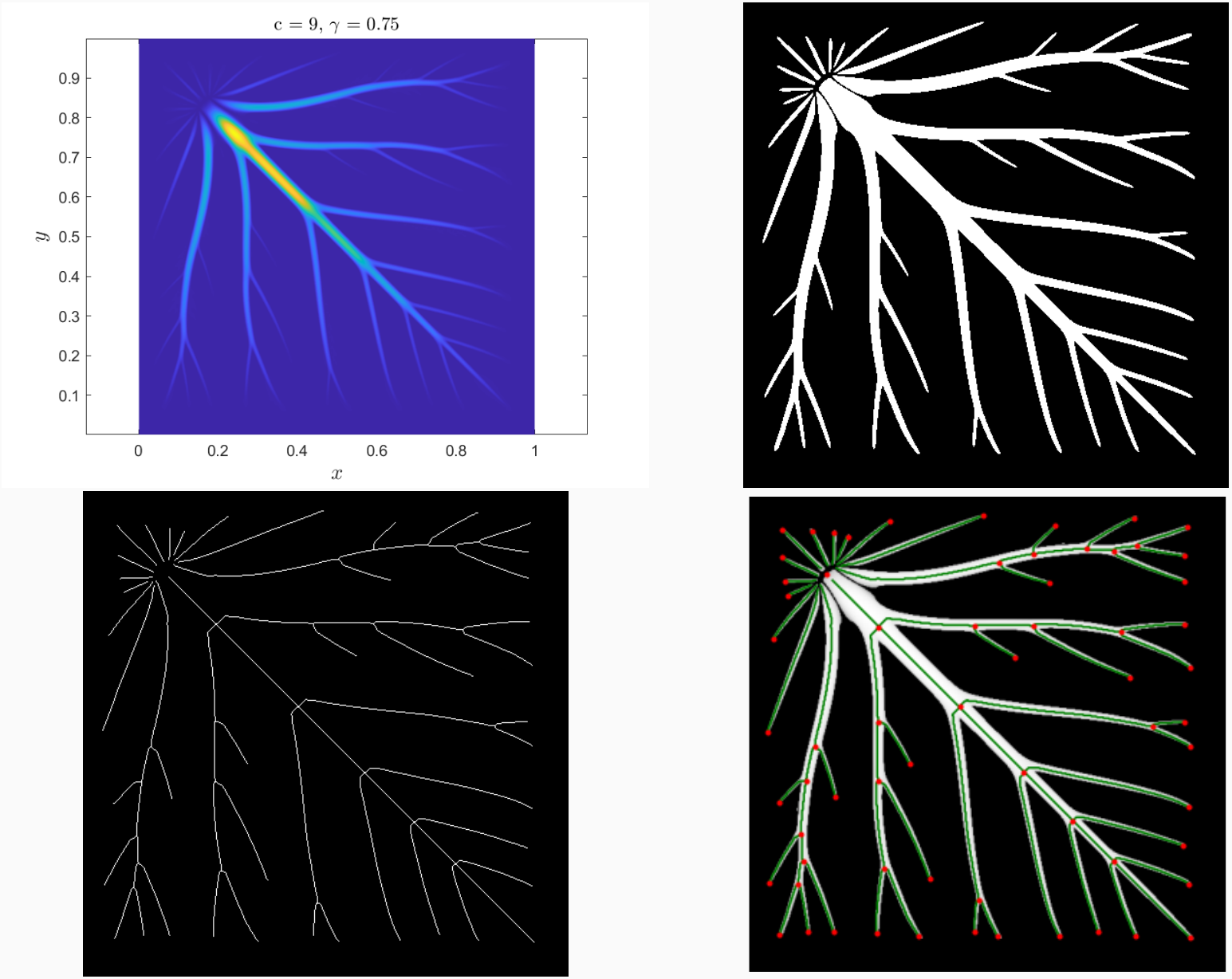

Figure 13: *Segmentation for* $c = 9, \gamma = 0.75$.

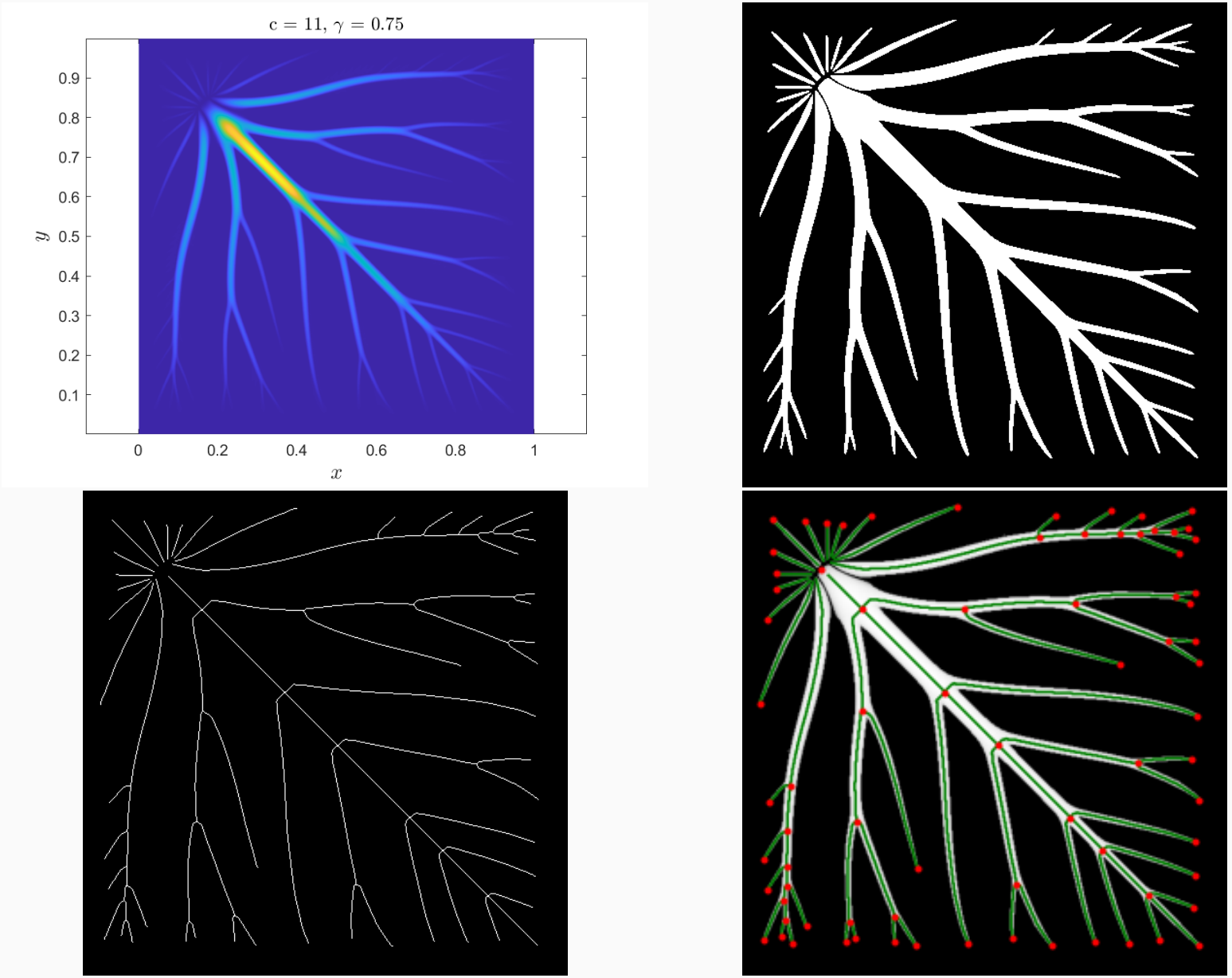

Figure 14: *Segmentation for* $c = 11, \gamma = 0.75$.

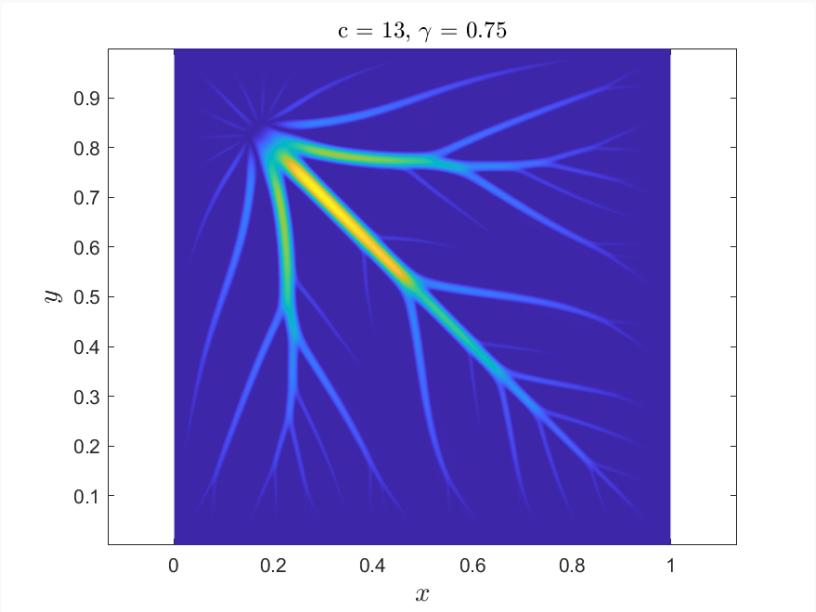

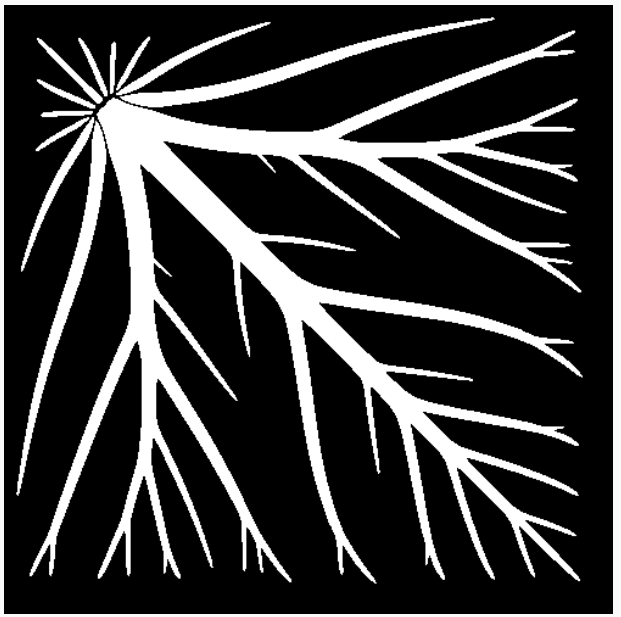

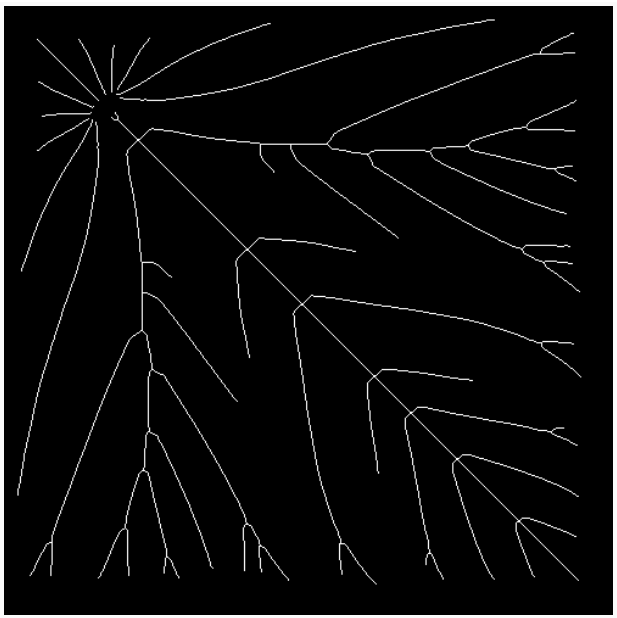

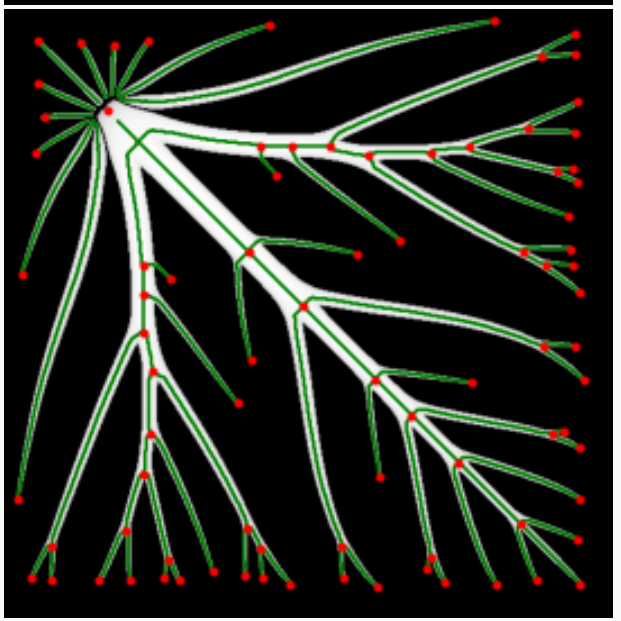

Figure 15: *Segmentation for* $c = 13, \gamma = 0.75$.

multiscale challenge: are $r = \varepsilon = 10^{-3}$ small enough?

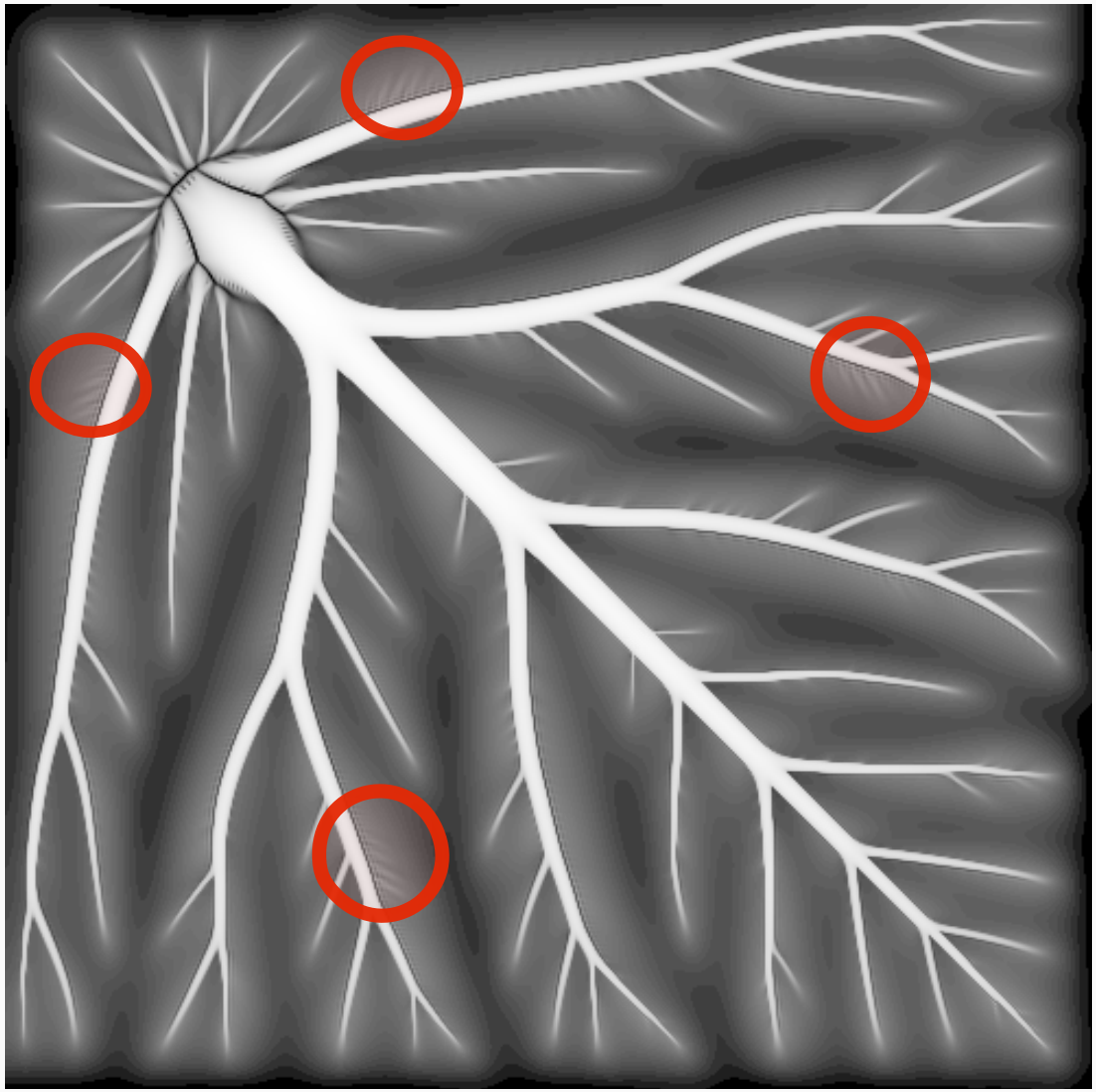

Figure 16: $c = 11, \gamma = 0.65$.

Future work and Conclusions

- $\surd$ comparison between vector and tensor model
- $\surd$ second order scheme in space and time with Wasserstein distance when $r \to 0$
- $\surd$ asymmetry related to the conditioning of the elliptic operator
- $\surd$ graph generation, starting from the numerical solutions of the system

Future work and Conclusions

- $\surd$ comparison between vector and tensor model
- $\surd$ second order scheme in space and time with Wasserstein distance when $r \to 0$
- $\surd$ asymmetry related to the conditioning of the elliptic operator
- $\surd$ graph generation, starting from the numerical solutions of the system
- ? efficient parallel solver to obtain very detailed solutions (working in progress with A. Coco)
- ? clustering (to find out to which plant the leaf belongs)

clustering ?

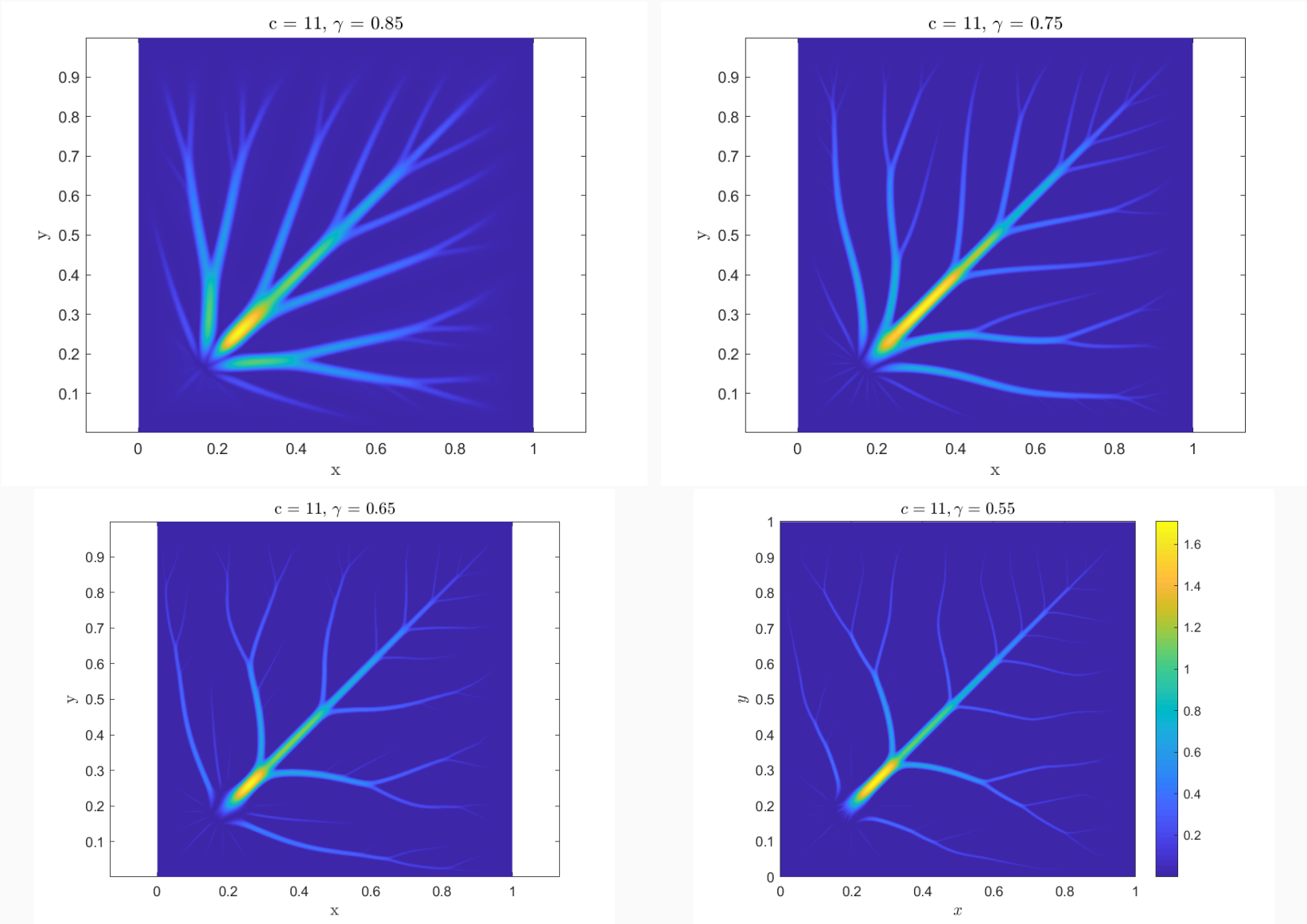

Figure 17: *Plot of $|\mathbb{C}|$ for different values of γ.*

Future work

? leaf venation has a large number of closed loops, which are functional and able to transport fluid in the event of damage to any vein, including the primary veins

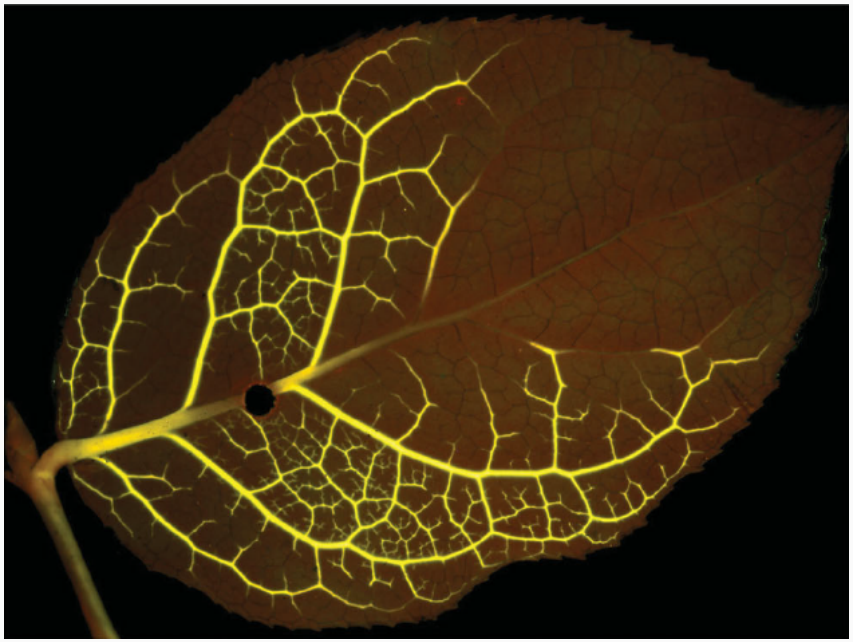

Thank you for the attention